Theoretical Chemistry Accounts (2020) 139:23
https://doi.org/10.1007/s00214-020-2544-9

REGULAR ARTICLE

3*d*-transition metals (Cu, Fe, Mn, Ni, V and Zn)-doped pentacene π-conjugated organic molecule for photovoltaic applications: DFT and TD-DFT calculations

İskender Muz[1] · Fahrettin Göktaş[2] · Mustafa Kurban[3]

Received: 23 October 2019 / Accepted: 6 January 2020 / Published online: 9 January 2020

Abstract
In this study, we have performed a thorough examination of density functional theory (DFT) and time-dependent (TD) DFT to investigate the structural and optoelectronic properties of 3*d*-transition metals (Cu, Fe, Mn, Ni, V and Zn)-doped pentacene π-conjugated organic molecule. The HOMO energy level of Ni-doped pentacene is −6.17 eV wide, i.e., about 1.31 eV greater and more negative than pentacene. The bandgap of the pentacene considerable decreases from 2.20 eV to 1.32, 1.35 and 0.37 eV, for Mn, Zn and V-doped pentacene structures, respectively, which affords an efficient charge transfer from HOMO to LUMO. The HOMO–LUMO energy gap is higher (4.44 eV, for Ni-doped pentacene), implying that the kinetic energy is higher and high chemical reactivity. We have examined, additionally, the reactivity and absorption properties of individual undoped and 3*d*-transition metals-doped pentacene. Pentacene has the largest vertical ionization potential (6.18 eV), corresponding to the highest chemical stability. Our results suggest that the new 3*d*-transition metals-doped pentacene may significantly contribute to the efficiency of solar cells.

Keywords Pentacene · 3*d*-transition metals · Bandgap · TD-DFT

1 Introduction

After it was proved that doped organic molecules were electrically conductive and some were even superconductive [1], they attracted an enormous interest regarding their use for molecular electronics. Especially, π-conjugated organic molecules were used in organic electronics such as organic field-effect transistors (OFETs) and organic photovoltaic (OPV) devices [2–4]. These molecules present unique properties suitable to the highest occupied molecular orbital (HOMO), the lowest unoccupied molecular orbital (LUMO) and HOMO–LUMO gaps. Furthermore, their photo-physical properties can be tuned allowing to design molecules via the donor–acceptor architecture [5, 6].

As one of the examples of π-conjugated organic compounds, pentacene ($C_{22}H_{14}$)—a polycyclic aromatic hydrocarbon—is a promising candidate for OPV devices [7]. Because it has a high field effect, electron and hole mobility and low bandgap properties [8–12], it can be used to form bilayer junctions with C_{60} and perylene [13–18] in manufacturing efficient organic, dye-sensitized [19] and polymer solar cells [20]. Pentacene is an electron-donor organic material that can be used in OFETs [21] and modified for the development of solution processability [22–24]. The derivatives of pentacene include desirable properties for organic thin-film transistors (OTFTs). They are used as n-type organic semiconductors in OTFTs with high electron mobility [25], in OFETs due to having a low bandgap, large π-conjugated system, and exhibit good solubility and stability [26]. Thus, in molecular crystals of aromatic molecules like pentacene the energetic properties such as the binding energy, the ionization potential (IP), the electron affinity (EA), the HOMO, LUMO, HOMO–LUMO gaps and the valence band width are important for understanding the charge transport mechanism. In a recent study, it

✉ Mustafa Kurban
mkurbanphys@gmail.com

[1] Department of Mathematics and Science Education, Nevşehir Hacı Bektaş Veli University, 50300 Nevşehir, Turkey

[2] Department of Energy System Engineering, Ankara Yıldırım Beyazıt University, 06170 Ankara, Turkey

[3] Department of Electronics and Automation, Kırşehir Ahi Evran University, 40100 Kırşehir, Turkey

was demonstrated that structural modification of pentacene monomers with diacid molecules can be used as a donor for bulk heterojunction (BHJ) solar cells [27]. Moreover, an experimental study has been carried out on Mg-doped pentacene. In the study, it has been found that using Mg as a dopant provides novel physical characteristics previously not encountered in organic field-effect transistors based on pentacene [28].

Our motivation for further investigation functionalized pentacene for designing BHJ solar cells. Thus, in this study, our aim is to investigate structural and optoelectronic properties such as binding energy, ionization potential, electron affinity, chemical hardness, HOMO–LUMO gap, refractive index, electrophilicity index, chemical potential, the maximum amount of electronic charge index and UV–vis spectra of 3*d*-transition metals (TM) (Cu, Fe, Mn, Ni, V and Zn)-doped pentacene as a potential material for photovoltaic applications. Herein, we are interested in theoretical investigation of *3d*-transition metals-doped pentacene because theoretical calculation could predict the advantages and disadvantages of new pentacenes in advance of the synthetic works. In this work, we used pentacene as a model system and systematically investigated the influence of Cu, Fe, Mn, Ni, V and Zn atoms on its optical and charge transport properties.

2 Computational methodology

To model the pentacene compounds, a pure pentacene compound was initially optimized at the B3LYP/6-311G(d,p) level of theory. Then, two TM separately replaced two hydrogen atoms in the meso-point of pentacene as in the TIPS-pentacene compound (see Fig. 1). Doping strategy has been widely used in oligoacenes with different types of atoms such as B, P, S, O and N. Among them, for example, P-doped pentacene on the meso-point in a symmetric way (among different 35 phosphapentacene derivatives) is the simplest example exhibits the smallest hole transport reorganization energy reported for heteropentacene derivatives up to today, and this compound could be a potential promising candidate in high-performance *p*-type OFET [29]. Besides, the HOMO–LUMO energy gap shows a large decrease from 2.19 eV for pentacene to 1.71 eV for P-doped pentacene on the meso-point in a symmetric way. The substitution of an atom or any molecule on pentacene on the meso-points in a symmetric way also displays higher charge carrier mobility [30]. All calculations were carried out using DFT calculations based on the B3LYP exchange–correlation functional with 6-311G(d,p) basis set [31, 32] as implemented in the Gaussian 09 program [33].

Binding energy per atom of TM-doped pentacene compounds was calculated by the following formula:

$$E_{\mathrm{b}}\left[\text{pen-TM}\right] = (22 \times E[\mathrm{C}] + 12 \times E[\mathrm{H}] + 2 \times E[\mathrm{TM}] - E\left[\text{pen-TM}\right])/36 \quad (1)$$

where E[C], E[H] and E[TM] represent the individual energies of C, H and TM atoms, respectively. The numbers in Eq. (1) show that there are 22 C atoms, 12 H atoms and 2 TM atoms in the new pentacene. Also, the vertical ionization potential (VIP) and vertical electron affinity (VEA) of all optimized structures were calculated as follows:

$$\mathrm{VIP} = E_{\mathrm{cation}} - E_{\mathrm{neutral}} \quad (2)$$

$$\mathrm{VEA} = E_{\mathrm{neutral}} - E_{\mathrm{anion}} \quad (3)$$

where VIP and VEA are defined as the energy difference between the E_{cation} and E_{neutral} of the neutral optimized geometry and the energy difference between the E_{neutral} and E_{anion} of the neutral optimized geometry, respectively. To explain the molecular structure and chemical reactivity of the pentacene and TM-doped pentacene compounds, the quantum chemical descriptors such as chemical hardness (η), chemical potential (μ), electrophilicity index (ω) and maximum

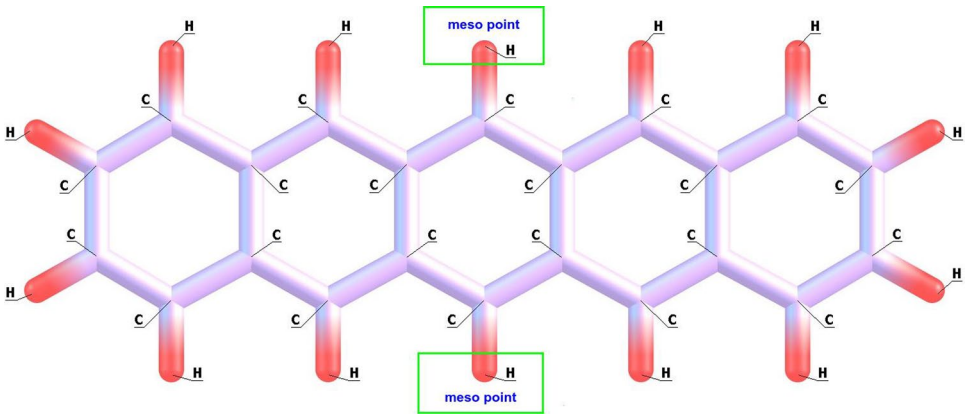

Fig. 1 The meso-points of pentacene

amount of electronic charge index $\left(N_{max}\right)$ were calculated by the following formulas [34, 35]:

$$\begin{aligned} &\left[\eta = (\mathrm{IP} - \mathrm{EA})/2\right], \quad \left[\mu = -(\mathrm{IP} + \mathrm{EA})/2\right] \\ &\left[\omega = \mu^2/2\eta\right] \quad \text{and} \quad \left[\Delta N_{max} = -\mu/\eta\right] \end{aligned} \tag{4}$$

where IP and EA correspond to ionization potential and electron affinity, respectively. According to Koopman's theorem, the energies of the HOMO and LUMO orbitals are given by IP $\approx -E_{HOMO}$ and EA $\approx -E_{LUMO}$. The natural bond orbital calculations were performed to understand both the charge distributions and the nature of donor–acceptor interactions. Time-dependent (TD) DFT calculation based on CAM-B3LYP functional [36] with 6-311G(d,p) basis set was performed for estimating absorption spectra because B3LYP underestimates excited state energies [37–39].

3 Results and discussions

3.1 Stability and structural properties

Figure 2 shows the optimized geometries of pentacene and TM-doped pentacene compounds as well as bond distances between C atoms and doped TMs. C–H bond lengths in the meso-point of pentacene are found to be 1.086 Å. Besides, the bond length of pentacene is in agreement with experimental values [40] and previous studies [41, 42]. When two TM replaced two hydrogen atoms in the meso-point of pentacene, bond lengths between TM and C atoms lie in the range of 1.732 and 2.076 Å. Binding energy per atom (E_b) calculated using the DFT-B3LYP method is shown in Fig. 3. E_b value of pentacene is found to be − 6.50 eV. The E_b values of pen-TM compounds are decreased and lie in the range of − 6.26 and − 6.45 eV when two TM replaced two hydrogen atoms in the pentacene compound. The pen-Zn compound has the smallest binding energy, so it is more unstable than the others. These results indicate that structural stability is slightly decreased with doping TM to pentacene.

3.2 Electronic and reactivity properties

To evaluate the electronic properties of pentacene and TM-doped pentacene compounds, HOMO and LUMO energy gaps and levels are investigated in detail. The graph of HOMO and LUMO energy gap (E_g) is shown in Fig. 4. In this study, the calculated E_g value (2.20 eV) for the pentacene for B3LYP/6-311G(d,p) agrees with the experimental [43] value of 2.15 eV. The HOMO and LUMO energy gaps of pen-Fe, pen-Cu and pen-Ni are 3.51, 4.14 and 4.40 eV (see Table 1), respectively, indicating a low conductivity. However, the HOMO and LUMO energy gaps of pen-Mn, pen-Zn and pen-V are 1.32, 1.05 and 0.37 eV, respectively, indicating a high conductivity. These results indicate that pentacene is kinetically and thermally more stable than pen-Mn, pen-Zn and pen-V compounds. The HOMO and LUMO energy levels in the pen-V compound are − 3.72 and − 3.35 eV, respectively (see Fig. 5). pen-V has the smallest bandgap, so conductivity is higher than the others. We should also mention that the pen-V is the more proficient compound because the small bandgap easily makes the promotion of electrons in photovoltaics.

To carry out the reactivity properties of pentacene and TM-doped pentacene compounds, chemical hardness (η), chemical potential (μ), electrophilicity index (ω) and the maximum amount of electronic charge index (ΔN_{tot}) are investigated in detail. The values of η, μ, ω and ΔN_{tot} are listed in Table 1. The graph of η is also shown in Fig. 4. It is clearly seen that η illustrates a trend similar to the E_g graph. η values of pentacene and TM-doped pentacene compounds are found to be in the following decreasing order: pen-Ni > pen-Cu > pen-Fe > pen > pen-Mn > pen-Zn > pen-V. η value of pen-V is lower than that of other TM-doped pentacene compounds, thus indicating a lower resistance to charge transfer and change in the band structure.

VIP and *VEA* values as two important characteristics of the electronic structure are associated with the effects of electron donating and accepting, respectively. As shown in Table 1, the calculated *VIP* value (6.18 eV) for pentacene agrees with the experimental [44] value of 6.58 eV. VIP values of pen-TM compounds are sharply decreased from 6.18 to 1.91 eV due to two TM replaced two hydrogen atoms in the pentacene compound. On the other hand, VEA values are importantly increased from 1.35 eV to 4.44 eV when two TM atoms except for Cu replaced two hydrogen atoms in the pentacene compound.

Graphs of ω and ΔN_{tot} are shown in Fig. 6. ω values of pentacene, pen-Cu, pen-Fe and pen-Ni compounds lie in the range of 2.52 and 6.41 eV, whereas that of pen-Mn, pen-Zn and pen-V compounds lie in the range of 8.91 and 33.77. Similarly, ΔN_{tot} illustrates a trend similar to the ω graph. ΔN_{tot} values of pentacene and TM-doped pentacene compounds are found to be in the following increasing order: pen-Cu < pen-Ni < pen-Fe < pen < pen-Mn < pen-Zn < pen-V. All these results show that electron accepting for pen-Mn, pen-V and pen-Zn compounds is higher than the others.

3.3 Optical properties

In order to investigate the optical properties of pentacene and TM-doped pentacene compounds, refractive index and absorption spectra are investigated. Moss [45] found a relationship between the HOMO–LUMO gap $\left(E_g\right)$ and refractive index (n) in semiconductors as formalized as:

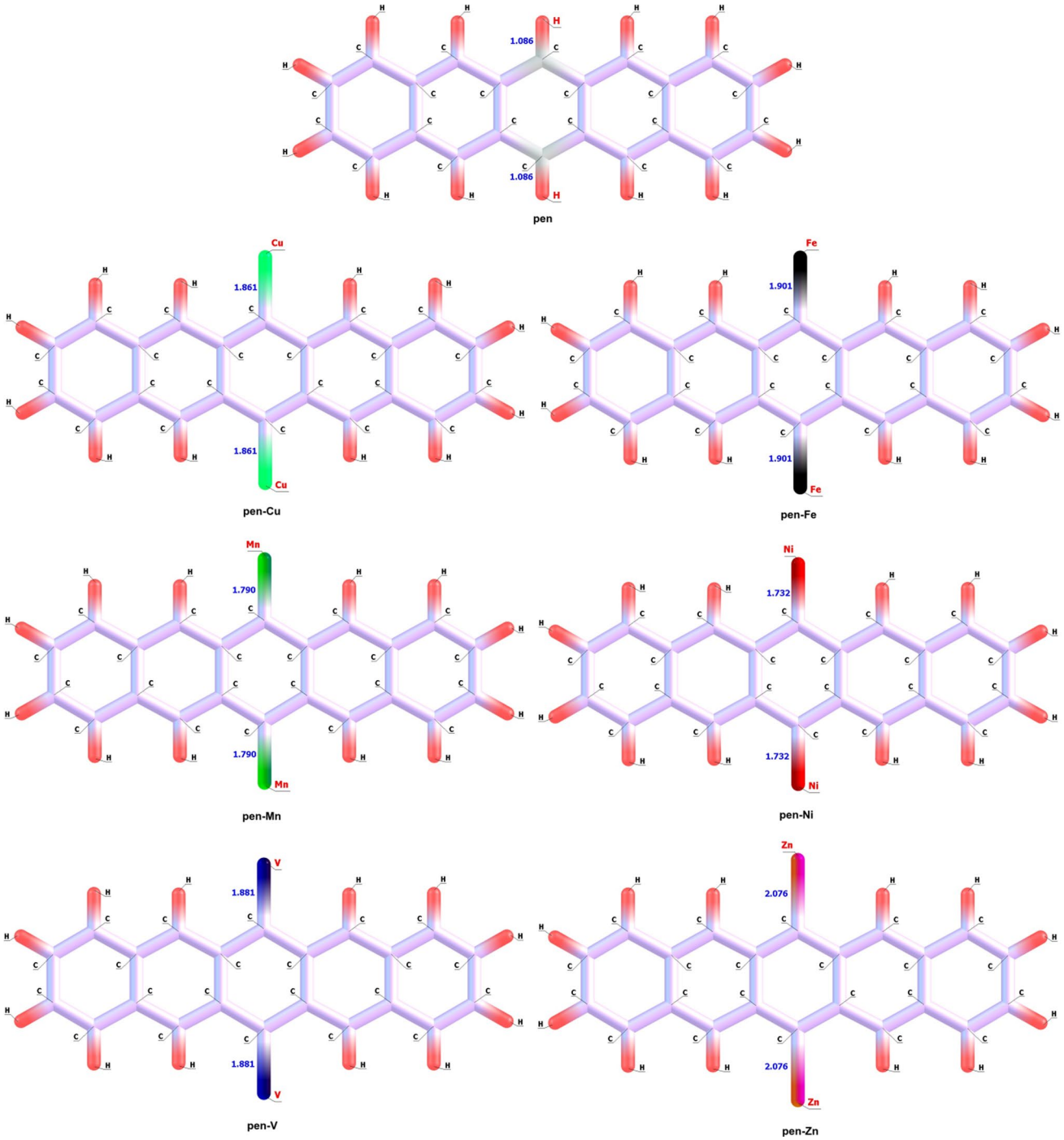

Fig. 2 The optimized geometries of pentacene and TM-doped pentacene compounds at the B3LYP/6-311G(d,p) level of theory

$$n^4 E_g = 95 \text{ eV} \tag{5}$$

The n of the pentacene and TM-doped pentacene compounds are calculated from Eq. 5, and the results are given in Table 2. The closest calculated n value (Moss relation) for pentacene (2.56) agrees with the experimental value 1.81. n values of pentacene lie also in the range of 2.56 and 2.72 eV. n values are decreased with doping Ni, Cu and Fe atoms, whereas they are increased with doping Mn, Zn and V atoms. We note that n values increase inversely based on a decrease in the energy band gaps from Eq. 5. This result indicates that there is a trend in a decrease in n values for Ni, Cu and Fe-doped pentacene, but an increase in n values for Mn, Zn and V-doped pentacene (see Table 2). Thus, pen-V

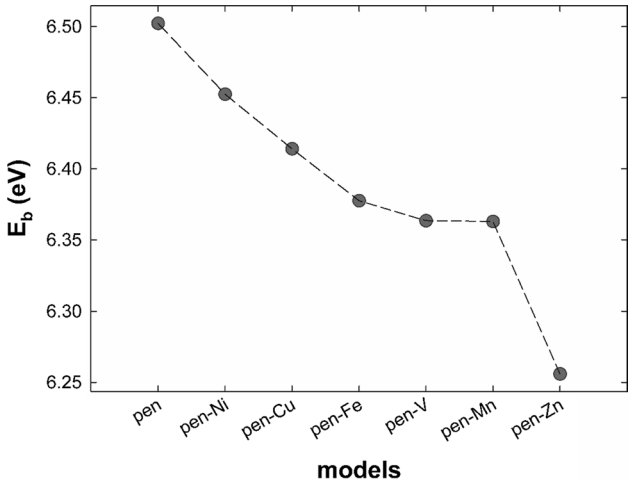

Fig. 3 Binding energy per atom (E_b) of pentacene and TM-doped pentacene compounds

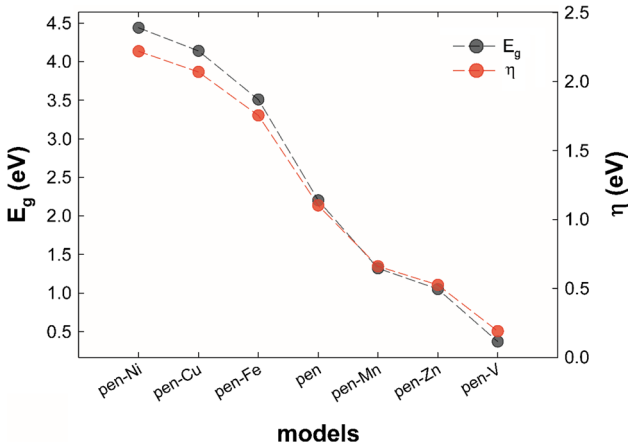

Fig. 4 The HOMO–LUMO energy gaps (E_g) and chemical hardness (η) of pentacene and TM-doped pentacene compounds

possesses the lowest bandgap, as well as broad and strong absorption in the visible.

Figure 7 displays the absorption spectra of undoped and TM-doped pentacene compounds. It was observed that there is an increasing trend in absorbance values in the range of 556–902 nm when it comes to Cu, Fe, Mn, Ni, V and Zn dopants. Especially, the Fe-doped pentacene structure needs the lowest energy (1.375 eV) in the absorbance maxima.

4 Conclusions

We performed a theoretical study to model the TM (Cu, Fe, Mn, Ni, V and Zn)-doped pentacene compounds as a material for organic photovoltaic devices. At that viewpoint, the structural, reactivity and optoelectronic properties such as binding energy, ionization potential, electron affinity, chemical hardness, HOMO–LUMO gap, refractive index, electronic charge index and absorption spectra of the pentacene compounds were investigated by DFT and TD-DFT calculations for the first time. Comparing with the pentacene compound, the pen-Mn, pen-Zn and pen-V compounds have more desirable properties. For instance, the pen-V compound is more conductive due to its smaller bandgap. The HOMO energy level of Ni-doped pentacene is − 6.17 eV wide, i.e., about 1.31 eV greater and more negative than pentacene. The bandgap of the pentacene considerably decreases from 2.20 eV to 1.32, 1.35 and 0.37 eV, for Mn, Zn and V-doped pentacene structures. There is a trend in a decrease in n values for Ni, Cu and Fe-doped pentacene, but an increase in n values for Mn, Zn and V-doped pentacene. Thus, pen-V possesses the lowest bandgap, as well as broad and strong absorption in the visible. We hope that the obtained results will provide an insight into experimental studies to design and produce various kinds of photovoltaic devices with higher efficiency based on the TM-doped pentacene.

Table 1 The electronic and reactivity properties of pentacene and TM-doped pentacene compounds

	pen	pen-Cu	pen-Fe	pen-Mn	pen-Ni	pen-V	pen-Zn
E_g	2.20	4.14	3.51	1.32	4.44	0.37	1.05
VIP	6.18	5.52	1.36	1.91	4.54	2.02	5.57
VEA	1.35	1.00	4.03	4.44	2.30	4.20	1.85
HOMO	− 4.86	− 5.30	− 5.86	− 4.09	− 6.17	− 4.84	− 4.20
LUMO	− 2.66	− 1.16	− 2.35	− 2.77	− 1.73	− 2.64	− 3.15
η	1.10	2.07	1.76	0.66	2.22	1.19	0.53
μ	− 3.76	− 3.23	− 4.11	− 3.43	− 3.95	− 3.54	− 3.68
ω	6.41	2.52	4.80	8.91	3.51	33.77	12.86
ΔN_{tot}	3.41	1.56	2.34	5.20	1.78	19.11	7.00

All values are in eV

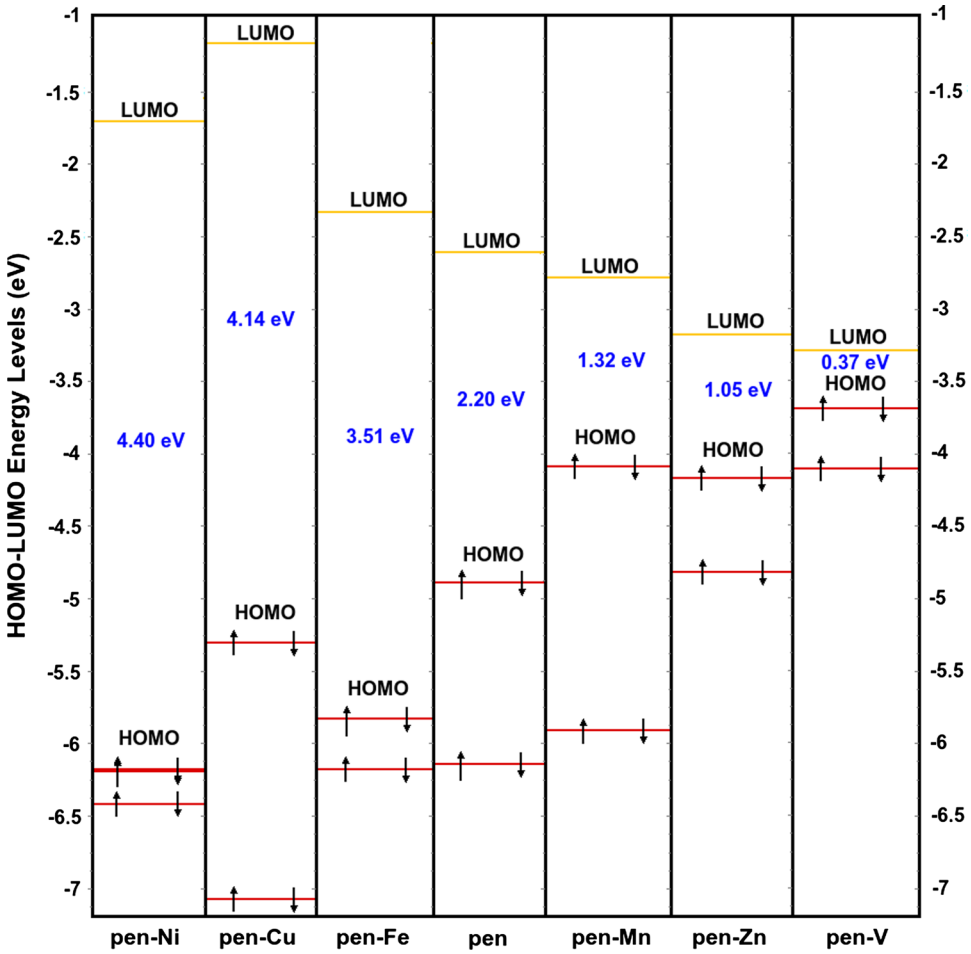

Fig. 5 The HOMO and LUMO energy levels of the pentacene and TM-doped pentacene compounds

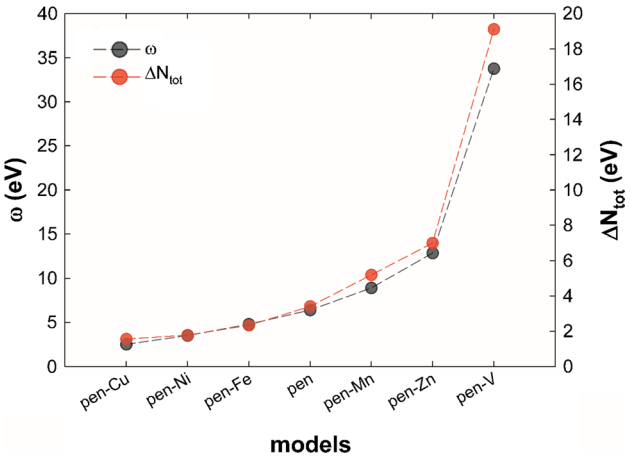

Fig. 6 The electrophilicity index (ω) and maximum amount of electronic charge index (ΔN_{tot}) of pentacene and TM-doped pentacene compounds

Table 2 The refractive indexes of pentacene and TM-doped pentacene compounds

	Herve-Vand.	Moss relation	Ravindra	Kumar-Singh	Exp.
pen-Ni	1.99	2.15	1.33	2.08	–
pen-Cu	2.05	2.19	1.52	2.13	–
pen-Fe	2.19	2.28	1.91	2.25	–
pen	2.60	2.56	2.72	2.61	1.81
pen-Mn	3.01	2.91	3.27	3.08	–
pen-Zn	3.17	3.08	3.43	3.31	–
pen-V	3.68	4.00	3.85	4.64	–

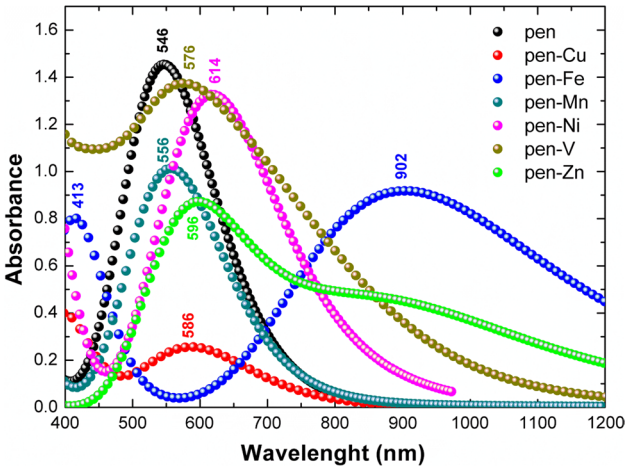

Fig. 7 The UV–vis spectra of pentacene and TM-doped pentacene compounds at the CAM-B3LYP/6-311G(d,p) level of theory

References

1. Rieger R, Kastler M, Enkelmann V, Müllen K (2008) Entry to coronene chemistry—making large electron donors and acceptors. Chem A Eur J 14:6322–6325. https://doi.org/10.1002/chem.200800832
2. Duan C, Zhang K, Zhong C, Huang F, Cao Y (2013) Recent advances in water/alcohol-soluble π-conjugated materials: new materials and growing applications in solar cells. Chem Soc Rev 42:9071–9104. https://doi.org/10.1039/C3CS60200A
3. Beaujuge PM, Fréchet JMJ (2011) Molecular design and ordering effects in π-functional materials for transistor and solar cell applications. J Am Chem Soc 133:20009–20029. https://doi.org/10.1021/ja2073643
4. Facchetti A (2011) π-conjugated polymers for organic electronics and photovoltaic cell applications. Chem Mater 23:733–758. https://doi.org/10.1021/cm102419z
5. Kitamura T, Ikeda M, Shigaki K, Inoue T, Anderson NA, Ai X, Lian T, Yanagida S (2004) Phenyl-conjugated oligoene sensitizers for TiO_2 solar cells. Chem Mater 16:1806–1812. https://doi.org/10.1021/cm0349708
6. Rieger R (2009) Extended donor and acceptor molecules for organic electronics. Dissertation on the degree "Doctor of Science", The Department of Chemistry, pharmacy and Geosciences Johannes Gutenberg—university Mainz
7. Lin YY, Gundlach DJ, Nelson SF, Jackson TN (1997) Pentacene-based organic thin-film transistors. IEEE Trans Electron Devices 44:1325–1331. https://doi.org/10.1109/16.605476
8. Nelson SF, Lin YY, Gundlach DJ, Jackson TN (1998) Temperature-independent transport in high-mobility pentacene transistors. Appl Phys Lett 72:1854–1856. https://doi.org/10.1063/1.121205
9. Dimitrakopoulos CD, Malenfant PRL (2002) Organic thin film transistors for large area electronics. Adv Mater 14:99–117. https://doi.org/10.1002/1521-4095(20020116)14:2%3c99:AID-ADMA99%3e3.0.CO;2-9
10. Chason M, Brazis PW, Zhang H, Kalyanasundaram K, Gamota DR (2005) Printed organic semiconducting devices. Proc IEEE 93:1348–1356. https://doi.org/10.1109/JPROC.2005.850306
11. Yang H, Shin TJ, Ling M-M, Cho K, Ryu CY, Bao Z (2005) Conducting AFM and 2D GIXD studies on pentacene thin films. J Am Chem Soc 127:11542–11543. https://doi.org/10.1021/ja052478e
12. Heringdorf F, Reuter MC, Tromp RM (2001) Growth dynamics of pentacene thin films. Nature 412:517–520. https://doi.org/10.1038/35087532
13. Yang J, Nguyen T-Q (2007) Effects of thin film processing on pentacene/C60 bilayer solar cell performance. Org Electron 8:566–574. https://doi.org/10.1016/j.orgel.2007.04.005
14. Nanditha DM, Dissanayake M, Hatton RA, Curry RJ, Silva SRP (2007) Operation of a reversed pentacene-fullerene discrete heterojunction photovoltaic device. Appl Phys Lett 90:113505. https://doi.org/10.1063/1.2713345
15. Pandey AK, Unni KNN, Nunzi J-M (2006) Pentacene/perylene co-deposited solar cells. Thin Solid Films 511–512:529–532. https://doi.org/10.1016/j.tsf.2005.12.015
16. Yoo S, Domercq B, Kippelen B (2004) Efficient thin-film organic solar cells based on pentacene/C60 heterojunctions. Appl Phys Lett 85:5427–5429. https://doi.org/10.1063/1.1829777
17. Yoo S, Domercq B, Kippelen B (2005) Intensity-dependent equivalent circuit parameters of organic solar cells based on pentacene and C60. J Appl Phys 97:103706. https://doi.org/10.1063/1.1895473
18. Pandey AK, Nunzi J-M (2006) Efficient flexible and thermally stable pentacene/C60 small molecule based organic solar cells. Appl Phys Lett 89:213506. https://doi.org/10.1063/1.2396927
19. Senadeera GKR, Jayaweera PVV, Perera VPS, Tennakone K (2002) Solid-state dye-sensitized photocell based on pentacene as a hole collector. Sol Energy Mater Sol Cells 73:103–108. https://doi.org/10.1016/S0927-0248(01)00143-X
20. Unni KNN, Pandey AK, Alem S, Nunzi J-M (2006) Ambipolar organic field-effect transistor fabricated by co-evaporation of pentacene and N,N′-ditridecylperylene-3,4,9,10-tetracarboxylic diimide. Chem Phys Lett 421:554–557. https://doi.org/10.1016/j.cplett.2006.01.113
21. Anthony JE (2008) The larger acenes: versatile organic semiconductors. Angew Chemie Int Ed 47:452–483. https://doi.org/10.1002/anie.200604045
22. Lloyd MT, Mayer AC, Tayi AS, Bowen AM, Kasen TG, Herman DJ, Mourey DA, Anthony JE, Malliaras GG (2006) Photovoltaic cells from a soluble pentacene derivative. Org Electron 7:243–248. https://doi.org/10.1016/j.orgel.2006.03.002
23. Lloyd MT, Mayer AC, Subramanian S, Mourey DA, Herman DJ, Bapat AV, Anthony JE, Malliaras GG (2007) Efficient solution-processed photovoltaic cells based on an anthradithiophene/fullerene blend. J Am Chem Soc 129:9144–9149. https://doi.org/10.1021/ja072147x
24. Palilis LC, Lane PA, Kushto GP, Purushothaman B, Anthony JE, Kafafi ZH (2008) Organic photovoltaic cells with high open circuit voltages based on pentacene derivatives. Org Electron 9:747–752. https://doi.org/10.1016/j.orgel.2008.05.015
25. Tang Q, Liang Z, Liu J, Xu J, Miao Q (2010) N-heteroquinones: quadruple weak hydrogen bonds and n-channel transistors. Chem Commun 46:2977. https://doi.org/10.1039/c001215g
26. Qu H, Shen H, Li J, Men Y, Chen X, Chong Z (2018) Synthesis and characterization of three pentacene derivatives. Trans Tianjin Univ 24:453–460. https://doi.org/10.1007/s12209-018-0136-8
27. Pramanik A, Sarkar S, Pal S, Sarkar P (2015) Pentacene–fullerene bulk-heterojunction solar cell: a computational study. Phys Lett A 379:1036–1042. https://doi.org/10.1016/j.physleta.2015.01.040
28. Pedersen TM (2008) Electronic structure of manganese doped pentacene. University of Saskatchewan
29. Long G, Yang X, Chen W, Zhang M, Zhao Y, Chen Y, Zhang Q (2016) "Doping" pentacene with sp(2)-phosphorus atoms: towards high performance ambipolar semiconductors. Phys Chem Chem Phys 18:3173–3178. https://doi.org/10.1039/c5cp06200d
30. Schweicher G, Olivier Y, Lemaur V, Geerts YH (2014) What currently limits charge carrier mobility in crystals of molecular

semiconductors? Isr J Chem 54:595–620. https://doi.org/10.1002/ijch.201400047
31. Becke AD (1993) A new mixing of Hatree–Fock and local density functional theories. J Chem Phys 98:1372–1377. https://doi.org/10.1063/1.464304
32. Lee C, Yang W, Parr RG (1988) Development of the colle-salvetti correlation-energy formula into a functional of the electron density. Phys Rev B 37:785–789. https://doi.org/10.1103/PhysRevB.37.785
33. Frisch MJ, Trucks GW, Schlegel HB, Scuseria GE, Robb MA, Cheeseman JR, Scalmani G, Barone V, Mennucci B, Petersson GA, Nakatsuji H, Caricato M, Li X, Hratchian HP, Izmaylov AF, Bloino J, Zheng G, Sonnenberg JL, Hada M, Ehara M, Toyota K, Fukuda R, Hasegawa J, Ishida M, Nakajima T, Honda Y, Kitao O, Nakai H, Vreven T, Montgomery JA, Peralta JE, Ogliaro F, Bearpark M, Heyd JJ, Brothers E, Kudin KN, Staroverov VN, Kobayashi R, Normand J, Raghavachari K, Rendell A, Burant JC, Iyengar SS, Tomasi J, Cossi M, Rega N, Millam JM, Klene M, Knox JE, Cross JB, Bakken V, Adamo C, Jaramillo J, Gomperts R, Stratmann RE, Yazyev O, Austin AJ, Cammi R, Pomelli C, Ochterski JW, Martin RL, Morokuma K, Zakrzewski VG, Voth GA, Salvador P, Dannenberg JJ, Dapprich S, Daniels AD, Farkas JB, Foresman JV, Ortiz J, Cioslowski DJ Fox (2009) Gaussian 09, Revision E.01. Gaussian Inc., Wallingford
34. Pearson RG (1993) The principle of maximum hardness. Acc Chem Res 26:250–255. https://doi.org/10.1021/ar00029a004
35. Parr RG, Pearson RG (1983) Absolute hardness—companion parameter to absolute electronegativity. J Am Chem Soc 105:7512–7516. https://doi.org/10.1021/ja00364a005
36. Yanai T, Tew DP, Handy NC (2004) A new hybrid exchange–correlation functional using the Coulomb-attenuating method (CAM-B3LYP). Chem Phys Lett 393:51–57. https://doi.org/10.1016/j.cplett.2004.06.011
37. Muz İ, Kurban M (2019) Enhancement of electronic, photophysical and optical properties of 5,5′-Dibromo-2,2′-bithiophene molecule: new aspect to molecular design. Opto-Electron Rev 27:113–118. https://doi.org/10.1016/j.opelre.2019.03.002
38. Kurban M (2018) Electronic structure, optical and structural properties of Si, Ni, B and N-doped a carbon nanotube: DFT study. Optik (Stuttg) 172:295–301. https://doi.org/10.1016/j.ijleo.2018.07.028
39. Gunduz B, Kurban M (2018) Photonic, spectroscopic properties and electronic structure of PTCDI-C8 organic nanostructure. Vib Spectrosc 96:46–51. https://doi.org/10.1016/j.vibspec.2018.02.008
40. Campbell RB, Robertson JM, Trotter J (1961) The crystal and molecular structure of pentacene. Acta Crystallogr 14:705–711. https://doi.org/10.1107/S0365110X61002163
41. Dierksen M, Grimme S (2004) Density functional calculations of the vibronic structure of electronic absorption spectra. J Chem Phys 120:3544–3554. https://doi.org/10.1063/1.1642595
42. Kadantsev ES, Stott MJ, Rubio A (2006) Electronic structure and excitations in oligoacenes from ab initio calculations. J Chem Phys 124:134901. https://doi.org/10.1063/1.2186999
43. Maliakal A, Raghavachari K, Katz H, Chandross E, Siegrist T (2004) Photochemical stability of pentacene and a substituted pentacene in solution and in thin films. Chem Mater 16:4980–4986. https://doi.org/10.1021/cm049060k
44. Gruhn NE, da Silva DA, Bill TG, Malagoli M, Coropceanu V, Kahn A, Bredas JL (2002) The vibrational reorganization energy in pentacene: molecular influences on charge transport. J Am Chem Soc 124:7918–7919. https://doi.org/10.1021/ja0175892
45. Moss TS (1985) Relations between the refractive index and energy gap of semiconductors. Phys Status Solidi 131:415–427. https://doi.org/10.1002/pssb.2221310202